IEEE Access
Multidisciplinary | Rapid Review | Open Access Journal

Received June 15, 2018, accepted August 15, 2018, date of publication August 28, 2018, date of current version September 28, 2018.

Digital Object Identifier 10.1109/ACCESS.2018.2867560

Universal Adaptive Stabilizer Based Optimization for Li-Ion Battery Model Parameters Estimation: An Experimental Study

HAFIZ M. USMAN, SHAYOK MUKHOPADHYAY, AND HABIBUR REHMAN
Department of Electrical Engineering, American University of Sharjah, Sharjah 26666, United Arab Emirates

Corresponding author: Shayok Mukhopadhyay (smukhopadhyay@aus.edu)

This work was supported in part by the Office of Research and Graduate Studies at the American University of Sharjah under Grant FRG-17-R34 and in part by the Department of Electrical Engineering.

ABSTRACT This paper proposes a two-stage universal adaptive stabilizer (UAS)-based optimization technique for an accurate and efficient estimation of Li-ion battery model parameters. The first stage utilizes an UAS-based adaptive parameters estimation (APE) technique to acquire an initial estimate of battery model parameters. The second stage utilizes one of the three different optimization techniques, i.e., *fmincon*, particle swarm optimization (PSO), and hybrid PSO to improve the accuracy of battery model parameters obtained by the APE. The parameters estimated by the APE help in reducing the search space interval required by the optimization technique, thus reducing the computation time of the optimization process. Intensive computer simulation and experimentation are performed to estimate the battery terminal voltage using the estimated parameters. The accuracy of estimated battery parameters is evaluated by comparing the estimated and measured battery terminal voltage. The results show that the accuracy of the battery model parameters obtained by the optimization techniques alone is poor, and the required computation time is high. The accuracy of parameters obtained by UAS-based APE is good with very low computation time, while it is best when UAS-based APE is used in combination with the PSO, or hybrid PSO optimization techniques while requiring an intermediate amount of computation time.

INDEX TERMS Adaptive parameters estimation, Li-ion battery, particle swarm optimization, universal adaptive stabilizer.

I. INTRODUCTION

An accurate state of charge (SoC) estimation is critical for the battery energy management and protection. SoC plays a vital role in assessing remaining battery lifetime, protection against overcharging and accidental over-discharging, fault detection and for a safe and reliable operation of a Li-ion battery [1]. Different algorithms for the SoC estimation are reviewed in [2]. Precise estimation of a battery SoC requires an accurate battery model. Electro-chemical [3] and mathematical models [4] of a battery are complex and can be computationally expensive. The battery model in [5] presents an equivalent circuit model of a battery which provides real time voltage, current dynamics, and all other essential dynamic characteristics. The battery model in [5] is utilized in this work because this model captures the effect of variation of SoC on the battery model parameters. Also as mentioned in [1], the model from [5] can incorporate effects of temperature, and number of charge-discharge cycles. Therefore, it is simple enough to be easily implemented for control oriented purposes, while it is detailed enough to capture essential dynamic characteristics. However, the method suggested in [5] requires a lot of experimental effort to acquire battery model parameters. Our earlier work [1] proposed an adaptive methodology for the parameters estimation of the model suggested in [5], which reduces experimental effort. The main contribution of the present work is a two-stage Li-ion battery model parameters estimation methodology. The proposed methodology increases the accuracy of the estimated battery model parameters, and battery terminal voltage estimation. It is also shown that the proposed battery model parameters estimation methodology reduces the computation time compared to using purely optimization based methods, and increases accuracy compared to the purely adaptation based method presented in [1].

A recently developed sensitivity-based group-wise Li-ion battery parameters estimation strategy is reported in [6]. The term sensitivity of a parameter quantifies the significance of a parameter on the output of Li-ion battery model.

In [6], the parameters having similar sensitivities are identified and grouped together using sensitivity analysis and are then identified by using the Levenberg-Marquardt algorithm. Wang and Li [7] propose a generic approach to estimate the Li-ion battery model parameters by utilizing the Particle Swarm Optimization (PSO) strategy. The algorithm for Li-ion battery parameters estimation using a Butterworth filter is outlined in [8]. The estimation of SoC and temperature dependent parameters of a Li-ion battery by Gauss-Newton and PSO techniques is studied in [9]. Battery model parameters are obtained experimentally via discharge data interpolation in [10]. A multi-objective optimization strategy to estimate equivalent circuit model battery parameters is analyzed in [11]. Non-linear least squares based battery parameters identification is reported in [12]. Genetic algorithm (GA) based optimization is used in [13] for battery parameters identification. But a GA is based on heuristics, and convergence for a GA based optimizer may take a very long time, and still may converge to a local optimum. Co-evolutionary particle swarm optimization PSO has been developed in [14] for optimum battery model parameters estimation. In [14], each battery parameter is optimized separately and the acquired optimized battery parameters are utilized in sequence, to get the optimal solution for the remaining parameters. The results obtained in [14] are accurate but the process is computationally time consuming. The PSO strategy is used in [15] to estimate an electrochemical Li-ion battery model's parameters. A study on convergence and stability analysis of the PSO algorithm is reported in [16]. Extended Levenberg-Marquart based optimization is used [17] to estimate Li-ion electrical circuit model parameters.

The combination of two or more strategies may produce accurate estimates of Li-ion battery parameters, but this may increase computational time [6], [9]. Furthermore, most of the optimization based Li-ion battery parameters estimation approaches are unguided, i.e. the search space, or search interval is selected randomly. The optimization techniques in [7], [9], [14] and [15] may substantially prolong the time required to obtain battery parameters, when initialized with random initial guesses, and randomly selected search intervals for battery parameters. In contrast our previous work [1] developed an adaptive parameter estimation (APE) technique which converges fast, with reasonable accuracy, and requires low computational time to estimate Li-ion battery parameters. However, the initial parameter values and their respective upper and lower bounds required by the APE technique can affect the accuracy of parameters and thus the accuracy of terminal voltage estimation.

This paper develops a two stage strategy for battery model parameters estimation. The APE process, which is the first stage of the proposed battery parameters estimation technique, helps in narrowing the search space for an optimizer i.e. the second stage of the proposed technique. This allows the optimization technique to quickly converge as compared to initializing an optimization routine with arbitrary guesses of initial conditions, and arbitrary search intervals. Compared to parameters estimation done by using APE alone, the proposed strategy minimizes the influence of initial guesses of parameters and their upper, lower bounds. Initial simulation results of this technique using only one optimization routine have been shared in [18]. The current paper provides detailed experimental results related to charging and discharging of batteries, and also considers three different optimization routines following the adaptive estimation process, and further provides a comprehensive analysis of battery parameters estimation accuracy, and the computation time required by each approach.

The organization of this paper is as follows. The background of the APE strategy and optimization routines used in this work is provided in Section II. Section III describes the proposed two-stage technique for estimation of Li-ion battery parameters. Computer simulation results for battery model parameters estimates are provided in Section IV. Section V presents the experimental validation, while section VI gives the concluding remarks along with the contributions made by this paper.

II. BACKGROUND

This work utilizes Chen and Mora's equivalent circuit model [5] of the Li-ion battery. Subsection II.A presents Chen and Mora's equivalent circuit model of a Li-ion battery, which has been verified by rigorous experimentation in [5]. Subsection II.B presents the UAS based APE technique [1] which is used to obtain estimated values of the Chen and Mora's battery model parameters. Finally, subsection II.C presents the optimization techniques [19] that are employed to improve the accuracy of the battery model parameters estimated by UAS based APE.

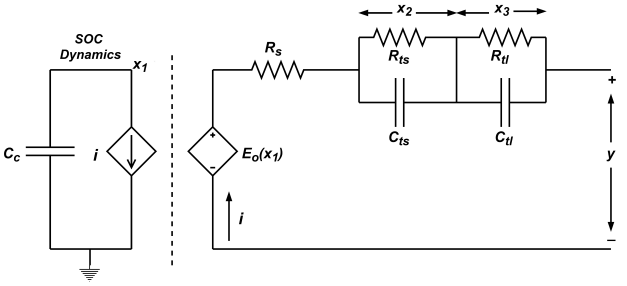

FIGURE 1. Equivalent circuit model used for Li-ion battery.

A. EQUIVALENT CIRCUIT MODEL OF A Li-ION BATTERY

The equivalent circuit model [5] of a Li-ion battery is shown in Fig. 1. This equivalent circuit model is easy to simulate [1], [20], [21]. The equivalent circuit parameters of this model are non-linear functions of battery SoC. In this model, transient response is captured by the RC network as shown in Fig. 1. A voltage-controlled voltage source models the dependence of the open circuit voltage on the battery SoC. The state space equations for Fig. 1 are described by (1)-(4).

$$\dot{x}_1(t) = -\frac{1}{C_c} i(t), \quad C_c = 3600 C f_1 f_2 f_3 \tag{1}$$

$$\dot{x}_2(t) = -\frac{x_2(t)}{R_{ts}(x_1(t))C_{ts}(x_1(t))} + \frac{i(t)}{C_{ts}(x_1(t))} \quad (2)$$

$$\dot{x}_3(t) = -\frac{x_3(t)}{R_{tl}(x_1(t))C_{tl}(x_1(t))} + \frac{i(t)}{C_{tl}(x_1(t))} \quad (3)$$

$$y(t) = E_o(x_1(t)) - x_2(t) - x_3(t) - i(t)R_s(x_1(t)) \quad (4)$$

State $x_1 \in [0, 1]$ denotes battery SoC, x_2 and x_3 represent voltage across $R_{ts}\|C_{ts}$ and $R_{tl}\|C_{tl}$ respectively. Factors f_1, f_2 and f_3, with values in $[0, 1]$, account for effects due to temperature, charge-discharge cycles, and self-discharge respectively, which, for simplicity, are taken as 1 in this work. C_c is the Ampere-hour (Ah) capacity of a battery and $y(t)$ denotes battery terminal voltage. The SoC dependent battery equivalent circuit elements of Fig. 1 are presented by (5)-(10).

$$E_o(x_1(t)) = -p_1 e^{-p_2 x_1(t)} + p_3 + p_4 x_1(t) - p_5 x_1^2(t) + p_6 x_1^3(t) \quad (5)$$

$$R_{ts}(x_1(t)) = p_7 e^{-p_8 x_1(t)} + p_9 \quad (6)$$

$$R_{tl}(x_1(t)) = p_{10} e^{-p_{11} x_1(t)} + p_{12} \quad (7)$$

$$C_{ts}(x_1(t)) = -p_{13} e^{-p_{14} x_1(t)} + p_{15} \quad (8)$$

$$C_{tl}(x_1(t)) = -p_{16} e^{-p_{17} x_1(t)} + p_{18} \quad (9)$$

$$R_s(x_1(t)) = p_{19} e^{-p_{20} x_1(t)} + p_{21} \quad (10)$$

Voltage relaxation tests (see [1]) are required to obtain the open circuit voltage curve for a battery. After this, curve fitting is used to obtain the parameters $p_1, \ldots, p_6$ in (5). The parameters of (5), for a 4V, 275mAh Li-ion battery obtained via curve fitting in [1] are $p_1 = 1.031, p_2 = 35, p_3 = 3.685, p_4 = 0.2156, p_5 = 0.1178, p_6 = 0.3201$. The remaining Li-ion battery model parameters described by (6)-(9) are obtained by the APE technique (see [1]). After estimating the battery parameters $p_7, \ldots, p_{18}$ using APE method, the battery series resistance parameters p_{19}, p_{20} and p_{21} can be obtained from the $R_s(x_1(t))$ vs SoC curve using curve fitting as described in [1].

B. UAS BASED ADAPTIVE PARAMETER ESTIMATION

The Mittag-Leffler (ML) function [22] is described by (11).

$$E_\alpha(z) = \sum_{k=0}^{\infty} \frac{z^k}{\Gamma(k\alpha + 1)} \quad (11)$$

Where $\Gamma(z + 1) = z\Gamma(z), z > 0$ is the standard Gamma function. UAS strategies have employed the ML function as a Nussbaum switching function [23] because fast error convergence is observed. A Nussbaum function is a piecewise right continuous function $N(\cdot) : [k', \infty) \to \mathbb{R}, k_0 > k'$, if it satisfies (12) and (13), [24].

$$\sup_{k>k_0} \frac{1}{k - k_0} \int_{k_0}^{k} N(\tau) d\tau = +\infty \quad (12)$$

$$\inf_{k>k_0} \frac{1}{k - k_0} \int_{k_0}^{k} N(\tau) d\tau = -\infty \quad (13)$$

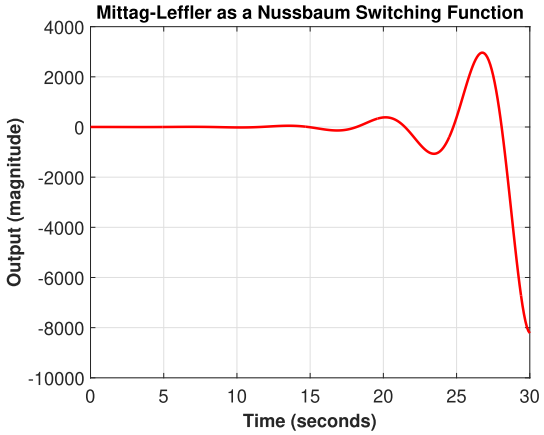

FIGURE 2. Mittag-Leffler function $E_\alpha(-\lambda t^\alpha)$ as a Nussbaum switching function for $\lambda = 1$ and $\alpha = 2.5$.

The ML function $E_\alpha(-\lambda t^\alpha)$ is a Nussbaum function if $\alpha \in (2, 3]$ and $\lambda > 0$ [25]. In this work, we select $\lambda = 1$ and $\alpha = 2.5$, a detailed examination of effects of α, λ are left for future efforts. The ML function is implemented as a Nussbaum switching function in MATLAB in [26] and an example is illustrated in Fig. 2. The circuit elements, described by (14)-(17), are estimated via the APE method using (19) which estimates the parameters $\widehat{p}_7, \ldots, \widehat{p}_{18}$. Where $\widehat{p}_n > 0$ for $n \in \{7, 8, \ldots, 18\}$. The adaptive equation (19) requires the steady-state upper, lower bounds and their respective confidence levels for each parameter.

$$\widehat{R}_{ts}(\widehat{x}_1(t)) = \widehat{p}_7 e^{-\widehat{p}_8 \widehat{x}_1(t)} + \widehat{p}_9 \quad (14)$$

$$\widehat{R}_{tl}(\widehat{x}_1(t)) = \widehat{p}_{10} e^{-\widehat{p}_{11} \widehat{x}_1(t)} + \widehat{p}_{12} \quad (15)$$

$$\widehat{C}_{ts}(\widehat{x}_1(t)) = -\widehat{p}_{13} e^{-\widehat{p}_{14} \widehat{x}_1(t)} + \widehat{p}_{15} \quad (16)$$

$$\widehat{C}_{tl}(\widehat{x}_1(t)) = -\widehat{p}_{16} e^{-\widehat{p}_{17} \widehat{x}_1(t)} + \widehat{p}_{18} \quad (17)$$

$$\widehat{R}_s(\widehat{x}_1(t)) = \widehat{p}_{19} e^{-\widehat{p}_{20} \widehat{x}_1(t)} + \widehat{p}_{21} \quad (18)$$

$$\dot{\widehat{p}}_n(t) = e^2(t) + \lambda_{x_n}(p_{nu} - \widehat{p}_n(t)) + \lambda_{y_n}(p_{nl} - \widehat{p}_n(t)) \quad (19)$$

The upper and lower bounds of the steady-state value of each parameter in (19) are p_{nu} and p_{nl} respectively; and λ_{xn}, λ_{yn} represent the confidence levels in upper and lower bounds respectively. The upper and lower bounds represent limits on the final steady-state value of the parameters $\widehat{p}_n$. The state space model given by (20)-(23), is a high-gain adaptive estimator used in the APE method. Where $\widehat{x}_1$ is the SoC, and is the same as x_1, $\widehat{x}_2$ and $\widehat{x}_3$ are the estimates of x_2 and x_3, and $\widehat{y}$ is the estimated battery terminal voltage.

$$\dot{\widehat{x}}_1(t) = -\frac{1}{C_c} i(t) \quad (20)$$

$$\dot{\widehat{x}}_2(t) = -\frac{\widehat{x}_2(t)}{\widehat{R}_{ts}(\widehat{x}_1(t))\widehat{C}_{ts}(\widehat{x}_1(t))} + u(t), \quad \widehat{x}_2(t) > 0 \quad (21)$$

$$\dot{\widehat{x}}_3(t) = -\frac{\widehat{x}_3(t)}{\widehat{R}_{tl}(\widehat{x}_1(t))\widehat{C}_{tl}(\widehat{x}_1(t))} + u(t), \quad \widehat{x}_3(t) > 0 \quad (22)$$

$$\widehat{y}(t) = \widehat{E}_o(\widehat{x}_1(t)) - \widehat{x}_2(t) - \widehat{x}_3(t) \quad (23)$$

The term $u(t)$ required by the observer equations (20)-(22) is calculated using (24)-(27).The error $e(t)$ between actual

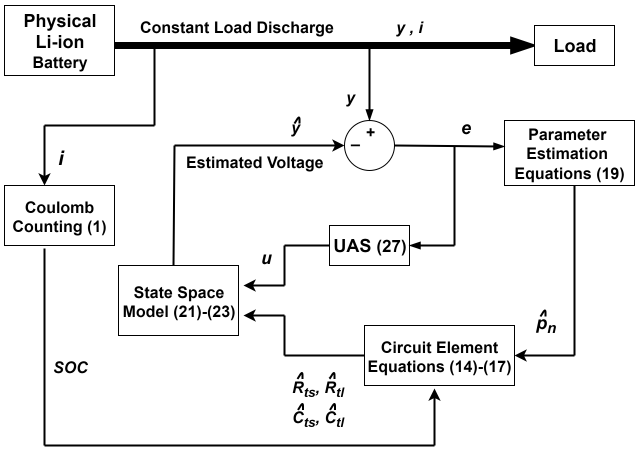

FIGURE 3. Adaptive parameter estimation methodology.

voltage $y(t)$, and estimated terminal voltage $\widehat{y}(t)$ is given by (24). The error $e(t)$ is used in (24) to adjust the growth rate of the adaptive gain i.e. $k(t)$. The value of λ and α in (26) are taken as 1 and 2.5 respectively.

$$e(t) = y(t) - \widehat{y}(t) \tag{24}$$
$$\dot{k}(t) = e^2(t), \quad k(t_0) = k_0 \tag{25}$$
$$N(k(t)) = E_\alpha(-\lambda k(t)^\alpha) \tag{26}$$
$$u(t) = -N(k(t))e(t) \tag{27}$$

The selection of initial guesses, upper, lower bounds with their respective confidence levels for each parameter according to the conditions described by (28)-(33) from [1] ensure the convergence of terminal voltage estimation error $e(t)$ to zero.

$$\widehat{p}_{13}(t_0) > \widehat{p}_{15}(t_0) > 0, \tag{28}$$
$$\lambda_{x_{15}} + \lambda_{y_{15}} > \lambda_{x_{13}} + \lambda_{y_{13}}, \tag{29}$$
$$\lambda_{x_{15}} p15_u + \lambda_{y_{15}} p15_l < \lambda_{x_{13}} p13_u + \lambda_{y_{13}} p13_l, \tag{30}$$
$$\widehat{p}_{16}(t_0) > \widehat{p}_{18}(t_0) > 0, \tag{31}$$
$$\lambda_{x_{18}} + \lambda_{y_{18}} > \lambda_{x_{16}} + \lambda_{y_{16}}, \tag{32}$$
$$\lambda_{x_{18}} p18_u + \lambda_{y_{18}} p18_l < \lambda_{x_{16}} p16_u + \lambda_{y_{16}} p16_l. \tag{33}$$

A very small positive discharge current needs to be maintained during the course of the APE process, which leads to the results as shown in (34)-(35), i.e. the products of estimated and actual battery equivalent circuit elements are equal [1].

$$\widehat{R}_{ts}(\widehat{x}_1(t))\widehat{C}_{ts}(\widehat{x}_1(t)) = R_{ts}(x_1(t))C_{ts}(x_1(t)) \tag{34}$$
$$\widehat{R}_{tl}(\widehat{x}_1(t))\widehat{C}_{tl}(\widehat{x}_1(t)) = R_{tl}(x_1(t))C_{tl}(x_1(t)) \tag{35}$$

The APE algorithm is shown in Fig. 3. For details related to the execution of the APE process, readers are requested to see [1].

C. PARTICLE SWARM OPTIMIZATION (PSO)

There are several ways to solve an optimization problem. This work uses three optimization techniques, i.e. *fmincon* from MATLAB, PSO, Hybrid PSO, either alone or in combination with adaptive parameters estimation. These optimization techniques are used at the second stage of the proposed battery parameters estimation methodology. The optimization function *fmincon* is a standard and widely used function readily available in the MATLAB optimization toolbox [27]. The description of Particle Swarm Optimization (PSO) is included in this work because it produces accurate results for our work. While Hybrid PSO is the combination of *fmincon* and PSO. Next we present the basics of PSO used in this work.

The key feature of PSO is that it is a non-gradient method which utilizes particles. For the work in this paper, the size of a particle is $1 \times n$ where $n = 15$, i.e. each element in the $1 \times n$ vector (forming a particle), represents one of the estimated Li-ion battery model parameters $\widehat{p}_7, \ldots, \widehat{p}_{21}$. The number of elements within a particle are called the decision variables, so for our $1 \times n$ vector of battery parameters a decision variable is a particular parameter i.e. $\widehat{p}_n$, $n \in \{7, \cdots, 21\}$. The upper and lower bounds for each decision variable (as stated in line-18 of Algorithm 1), swarm size S (i.e. number of particles), where $S \in \mathbb{Z}$, $S > 0$, and maximum number of iterations R also needs to be specified. In PSO terminology, a vector containing decision variables of the k^{th} particle, where $k \in \{1, \cdots, S\}$, is called the particle's position $d_k(t)$ at time t. A vector containing the values of the change in the values of the decision variables of this particle per time step, is called the particle's velocity $v_k(t)$ at time t. It is worth noting that the terms 'velocity' and 'position' of a particle are not necessarily equivalent to commonly known physical terms, but are more specifically defined via (36), and (37) respectively. The optimization process begins with the initialization of a particle's position, i.e. each decision variable in a particle is randomly assigned a number within the range specified by its lower bound and upper bound. Let $C(d_k(t))$ represents the cost function of the optimization problem, i.e. $C(d_k(t))$ needs to be minimized. In this work, $C(d_k(t)) = |e(t)|$, and $e(t)$ is given by (24). For all k particles, the cost function $C(d_k(t))$ is evaluated at each time step. For all $k \in \{1, \cdots, S\}$, let $d_{k_l}(t')$ be a particle having minimum cost $C(d_k(t'))$ for $t' \in [t_0, t]$, $k_l \in \{1, \cdots, S\}$. Further let $d_{k_g^*}(t^*)$ be a particle $d_{k_l}(t')$ with minimum cost $C(d_{k_l}(t'))$ over all k_l, $t^* \in [t_0, t]$. The particle $d_{k_l}(t')$ is said to have local best position in time interval $[t_0, t]$, and particle $d_{k_g^*}(t^*)$ is said to have global best position in interval $[t_0, t]$ and across all the swarms.

The velocity of each particle is set to zero at initialization, i.e. $v_k(t_0) = 0$. Further, $C(d_{k_l}(t_0))$ and $C(d_{k_g^*}(t_0))$ are assigned a very high value. The local best position of each particle at initial time is assigned as $d_{k_l}(t_0) = d_k(t_0)$. After the initialization, the new velocity and new position of each particle is found by using (36) and (37). The vector r_1 and r_2 have size $1 \times n$ and each element of vector r_1 and r_2 is a uniformly distributed random number within the range (0,1). Here m represents particle's inertia, $m \in (0, 1]$, and a smaller value of m usually provides less oscillations around a value at which a particle's decision variable converges. The weights assigned to local and global best positions are s_1 and s_2 respectively. The $\circ$ operator in (36) is the Hadamard product.

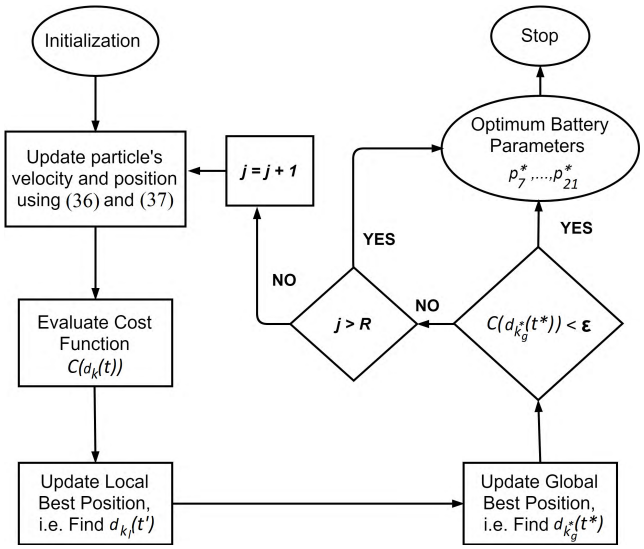

FIGURE 4. PSO Algorithm for optimum battery parameters estimation.

It is used for element wise multiplication of two vectors having the same sizes, i.e. the size of each vector is $1 \times n$. The resultant vector, obtained after element wise multiplication of two same sized vectors, has the size of $1 \times n$. Thus, the element wise multiplication of vectors in (36) gives the vector $v_k(t + \Delta t)$ of size $1 \times n$. The velocity and position of the k^{th} particle are updated continuously in a loop using (36) and (37) until $C(d_{k_g^*}(t^*))$ falls below a desired small positive value, say ϵ, or the number of iterations j exceeds the maximum value R, as shown in Fig. 4. Details related to the use of the PSO algorithm for estimating Li-ion battery parameters are presented in Section III. For details related to the PSO algorithm, readers are directed to [16] and [19].

$$v_k(t + \Delta t) = mv_k(t) + s_1 r_1 \circ (d_{k_l}(t') - d_k(t)) + s_2 r_2 \circ (d_{k_g^*}(t^*) - d_k(t)) \quad (36)$$

$$d_k(t + \Delta t) = d_k(t) + v_k(t + \Delta t) \quad (37)$$

In contrast to PSO, there are also gradient based optimization techniques, e.g. MATLAB's *fmincon* function provides an implementation of such gradient based optimization techniques. The combination of PSO and *fmincon* together is known as Hybrid PSO. In Hybrid PSO, the *fmincon* algorithm is executed on the output of the PSO algorithm, after the PSO algorithm terminates, to further refine the output produced by PSO. In this work we compare the results of applying the *fmincon*, PSO, and Hybrid PSO strategies as a second stage of the proposed UAS based optimized battery parameters estimation methodology. The proposed methodology is explained in the next section.

III. UAS BASED OPTIMIZED Li-ION BATTERY MODEL PARAMETERS ESTIMATION METHOD

This section explains the proposed adaptation based optimized strategy to estimate Li-ion battery model parameters. The left half of Fig. 5 shows the APE process. The formulation of the adaptive parameter estimation process is available in section II, and details are available in [1]. The process can be briefly described as follows. The adaptive parameters estimation process requires the open circuit voltage curve, which provides the value of the estimated open circuit voltage $\widehat{E}_0(\widehat{x}_1(t))$. This, along with the measured battery current $i(t)$, and the output $u(t)$ of the universal adaptive stabilizer, is used by the APE block to calculate the estimated battery terminal voltage $\widehat{y}(t)$. The difference between the measured battery terminal voltage $y(t)$, and $\widehat{y}(t)$ gives the terminal voltage estimation error $e(t)$. This error $e(t)$ is used to adaptively adjust values of the Li-ion battery model parameters. This process outputs parameters $\widehat{p}_7, \cdots, \widehat{p}_{18}$, which along with some further curve fitting based operations as shown in [1], produces parameters $\widehat{p}_{19}, \cdots, \widehat{p}_{21}$. The values of the battery terminal voltage $y(t)$, the battery current $i(t)$ at each time step of execution, and the values of estimated parameters $\widehat{p}_7, \cdots, \widehat{p}_{21}$ are stored in a data storage unit.

In the right half of Fig. 5, the dotted box represents the optimization process of the battery parameters obtained via UAS based estimation. The discrete data points i.e. the voltage and current data points stored in the data storage unit, are extracted by the data organizer block and forwarded to the sample and hold unit. The data organizer block also assigns the upper and lower bounds for battery parameters $\widehat{p}_7, \cdots, \widehat{p}_{21}$ required by optimization routine. The sample and hold block simply reads the terminal voltage and current values one by one, and holds them until one iteration of the optimization routine is completed. The optimization routine block also requires some constraints e.g. the number of iterations, number of swarms, upper and lower bounds of decision variable values, and desired minimum value for the cost function. The $\min_{t\in[t_0,T],k\in\{1,\cdots,S\}} C(x_{k_g^*}(t^*))$, where $t^* = [t_0, T], k_g^* \in \{1, \cdots, S\}$ optimization is then performed. Here T is the time at which battery SoC is 7%, $C(x_k(t)) = |e(t)|$, and $e(t)$ is given by (24). When the error $|e(t)|$ from cost function reaches a desired minimum value ϵ, the battery parameters $p_7^*, \cdots, p_{21}^*$ are recorded in arrays $B_7, \cdots, B_{21}$. When either the number of iterations or the minimum error criteria in estimated terminal voltage is satisfied, the iterator variable j is incremented to optimize the battery parameters at the next sample of voltage and current. The average of recorded battery parameters in $B_7, \cdots, B_{21}$ arrays, after the optimization process, provides the optimized estimates of Li-ion battery parameters and they are named as $\tilde{p}_7, \cdots, \tilde{p}_{21}$. The implementation details of the proposed technique, whose architecture is given in Fig 5, has been described in the Algorithm 1. It is also worth noting that T is selected as the time at which battery SoC is 7% [1] because it enables capturing battery behavior over a sufficiently long range of battery cycle life, while making sure that batteries are not discharged to dangerously low operating SoC.

The sampling time used to record Li-ion battery voltage and current should be appropriate enough to capture the nonlinear behavior of discharge voltage, especially for the range $7\% \leq \text{SoC} \leq 20\%$. We select the sampling time of 0.01 seconds for battery voltage and current sampling in

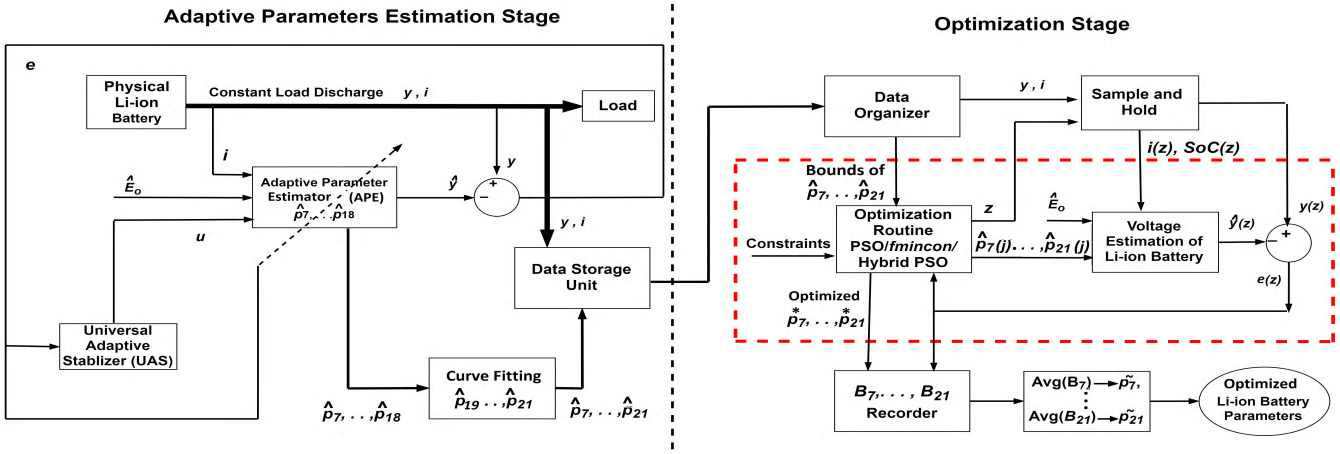

FIGURE 5. Architecture of APE followed by optimization methodology.

this work, which is sufficient enough to capture the nonlinear behavior of battery terminal voltage in the range of SoC mentioned above.

The factors influencing the computational time and accuracy of Algorithm 1 are as follows: 1. Sampling time of battery voltage and current, 2. Maximum number of optimization iterations, 3. Swarm size in optimization stage, 4. Search space interval for each decision variable in optimization stage, 5. Desired minimum value of cost function in optimization stage. The selection of these factors is a trade-off between more accurate estimates of Li-ion battery parameters and overall less computational time of Algorithm 1. Furthermore, the accuracy of Algorithm 1 has been observed to be more sensitive to factor 4 and 5 above, and the computational time relies mainly on factors 1, 2, and 3.

Our two-stage adaptive-optimized strategy focuses on optimum estimation of Li-ion battery parameters while reducing the number of iterations, number of swarms, and search space interval needed by the optimization technique. In the next section, we present a comprehensive comparison of accurate estimates of Li-ion battery parameters, and overall computational time between the APE technique, our proposed algorithm, and optimization routines.

IV. COMPUTER SIMULATIONS FOR BATTERY MODEL PARAMETERS ESTIMATION

The parameters of a 4.1 V, 850 mAh polymer Li-ion battery are obtained by Chen and Rincon-Mora in [5]. We used the same parameters as a benchmark to perform the computer simulations in this work. However, a Li-ion battery of 275 mAh capacity is used in this work to reduce the simulation time to almost one-third of the time needed, compared to using a 850 mAh Li-ion battery, which Chen and Mora utilize in their experiments. Note that the battery parameters of interest to this work are constants independent of SoC, and they control the shape of the terminal voltage vs time curve, thus reducing the capacity from 850mAh to 275 mAh doesn't affect the parameters of interest to this work. Three different techniques are used to estimate the battery parameters $\widehat{p}_7, \cdots, \widehat{p}_{21}$. In this work, these techniques will be termed as Technique 1 (T1), Technique 2 (T2), and Technique 3 (T3), and they are defined as follows.

- Technique 1 (T1): This technique utilizes one of the three optimization routines i.e. *fmincon* (T1-I), PSO (T1-II), and Hybrid PSO (T1-III). These optimization routines have a random search space interval for each parameter and number of iterations $R = 50$. A swarm size of $S = 50$ is set for PSO (T1-II) and Hybrid PSO (T1-III).
- Technique 2 (T2): This technique [1] uses Universal Adaptive Stabilizer (UAS) based Adaptive Parameters Estimation (APE) alone to acquire the set of Li-ion battery model parameters.
- Technique 3 (T3): This is our newly proposed technique which consists of a two-stage process. The first stage utilizes UAS based APE to obtain the initial values of the parameters. The second stage utilizes one of the three optimization routines i.e. *fmincon*, PSO, and Hybrid PSO. Thus, Technique 3 employs one of the three two-stage processes, i.e. APE with *fmincon* (T3-I), APE with PSO (T3-II), and APE with Hybrid PSO (T3-III). Complete details for the implementation of the proposed technique are given in the Algorithm 1. The search space interval, as defined in Algorithm 1, for each parameter is $\widehat{p}_7 \pm \delta_7, \ldots, \widehat{p}_{21} \pm \delta_{21}$. The values of parameters $\widehat{p}_7, \ldots, \widehat{p}_{21}$ are obtained from APE (T2) while the values of δ_n is set at 10 percent of the value of a parameter estimated by the APE process, i.e. $\delta_n = 0.1\widehat{p}_n$ and $n \in \{7, \cdots, 21\}$. The number of iterations for all optimization routines are $R = 10$ and swarm sizes of $S = 10$ are selected for PSO and Hybrid PSO. Please note that the number of iterations and swarm size are deliberately set to five times lesser than T1 to illustrate the effectiveness of the proposed technique T3.

The parameters estimated using techniques T1, T2, and T3 are first assessed by comparing the estimated battery

Algorithm 1 Adaptation, and optimization based Li-ion battery parameters estimation algorithm

Requirements: Current $i(t)$ and voltage $y(t)$ for battery discharge through a constant load resistance, where $t = [t_0, t_{end}]$ and t_{end} is the time at which battery SoC is 7%.

Data: Initial values $\widehat{p}_n(0) > 0$, $n \in \{7, \cdots, 18\}$, upper bounds p_{nu}, lower bounds p_{nl}, and their respective confidence levels λ_{x_n} and λ_{y_n} for each parameters $p_7, \ldots, p_{18}$. Battery capacity C_c (Ah) value. Maximum number of optimization iterations R, number of swarms S for PSO, and a small positive constant ϵ. Upper and lower limits of search space interval for optimization, i.e. $\widehat{p}_7 \pm \delta_7, \ldots, \widehat{p}_{21} \pm \delta_{21}$, where $\delta_n \in \mathbb{R}$, $n \in \{7, \cdots, 21\}$ and $\widehat{p}_7, \ldots, \widehat{p}_{21}$ obtained from APE.
Initial conditions $\widehat{x}_1(t_0) = 1, \widehat{x}_2(t_0) = \widehat{x}_3(t_0) = 0, \widehat{y}(t_0) = y(t_0)\,V$, and $SoC(t_0) = 1$. Initialize the iterator variables $h = 1$, $j = 1$, and $z = 1$.

Output: Optimized estimated battery model parameters $\tilde{p}_7, \ldots, \tilde{p}_{21}$.

for $t = t_0 : t_{step} : t_{end}$ **do** ▷ Adaptive parameters estimation of Li-ion battery.
  Read discharge current $i(t)$ and voltage $y(t)$.
  Update the error $e(t)$ using (24).
  Calculate battery $SoC(t)$ i.e. $x_1(t)$ using (1), and get $\hat{x}_1(t)$ using (20). ▷ Note that: $x_1(t) = \hat{x}_1(t)$.
  Get estimated parameters from (19).
  Find the equivalent circuit elements from (14) to (17).
  Evaluate state estimates from (21) and (22), and find estimated terminal voltage $\hat{y}(t)$ using (23).
  if $(|e(t)| < \epsilon)$ **then**
    Store the estimates of Li-ion battery parameters in arrays, $A_7[h] \leftarrow \widehat{p}_7(t), \cdots, A_{18}[h] \leftarrow \widehat{p}_{18}(t)$, and
    $h \leftarrow (h + 1)$.
  else
    Continue loop execution.
  end if
end for
Find the mean value of all individual arrays $A_7, \cdots, A_{18}$ to get the estimates of Li-ion battery parameters $\widehat{p}_7, \ldots, \widehat{p}_{18}$.
Estimate $\widehat{p}_{19}$, $\widehat{p}_{20}$ and $\widehat{p}_{21}$ parameters from $\widehat{R}_s(\widehat{x}_1(t))$ vs SoC curve using curve fitting as in [1].
Store all the battery parameters $\widehat{p}_7, \ldots, \widehat{p}_{21}$, voltage $y(t)$, current $i(t)$, and $SoC(t)$ profiles in the data storage unit.
Organize the data for optimization by setting upper and lower limits of search space interval for each parameter, i.e. $\widehat{p}_7 \pm \delta_7, \ldots, \widehat{p}_{21} \pm \delta_{21}$, where $\delta_n \in \mathbb{R}$, $n \in \{7, \cdots, 21\}$, and $\widehat{p}_7, \ldots, \widehat{p}_{21}$ obtained from APE.
while $SoC(z) > 7\%$ **do** ▷ Optimization of Li-ion battery model parameters.
  Read constant load discharge current *i(z)*, voltage *y(z)* and *SoC(z)* at z_{th} sample.
  Run an optimization routine (*fmincon*, PSO or Hybrid PSO) to identify the best value of battery parameters in the preset search space interval, i.e. get battery parameter values that minimize $|e(z)|$.
    ▷ The optimization process described in Fig. 4, along with (36) and (37), is used for APE with PSO (T3-II) or APE with Hybrid PSO (T3-III) techniques.
  if $(|e(z)| < \epsilon)$ **or** $(j > R)$ **then**
    Store the estimates of Li-ion battery parameters in arrays, $B_7[z] \leftarrow p_7^*(j), \cdots, B_{21}[z] \leftarrow p_{21}^*(j)$ and
    $j \leftarrow 1$ and $z \leftarrow (z + 1)$.
  else
    Continue $j \leftarrow (j + 1)$. ▷ Increment optimization algorithm iteration number.
  end if
end while
Find the mean value of all individual arrays $B_7, \cdots, B_{21}$ to get the optimized estimates of Li-ion battery parameters $\tilde{p}_7, \ldots, \tilde{p}_{21}$.

parameter values output by each of them, with the parameter values that were experimentally obtained by Chen and Mora. The computational time needed by each technique is also noted, and compared. Secondly, the values of battery circuit elements R_{ts}, R_{tl}, C_{ts}, C_{tl}, and R_s are calculated using the parameters $\widehat{p}_7, \ldots, \widehat{p}_{21}$. The values of these battery circuit elements are compared with the ones that are provided by Chen and Mora. Finally, the accuracy of the estimated parameters is evaluated by comparing the estimated battery terminal voltage using the above estimated battery parameters, with the battery terminal voltage given by Chen and Mora.

A. PARAMETERS ESTIMATION ACCURACY COMPARISON

The values of battery parameters $\widehat{p}_7, \ldots, \widehat{p}_{21}$ estimated by using three techniques, T1, T2, and T3 are given in Table-1.

TABLE 1. 4.1 V, 275 mAh Li-ion battery model parameters.

		Technique 1: $S = 50$ and $R = 50$			Technique 2	Technique 3: $S = 10$ and $R = 10$		
Parameters	Chen & Mora's model values	(T1-I) *fmincon*	(T1-II) PSO	(T1-III) Hybrid PSO	(T2) APE	(T3-I) APE with *fmincon*	(T3-II) APE with PSO	(T3-III) APE with Hybrid PSO
$\widehat{p}_7$	0.3208	9.5897	9.8156	9.7002	0.5555	0.4671	0.4269	0.4518
$\widehat{p}_8$	29.14	49.8232	52.6729	50.8992	29.9996	29.7794	28.9964	29.2309
$\widehat{p}_9$	0.0467	0.4188	0.4843	0.503	0.0552	0.0508	0.0476	0.0481
$\widehat{p}_{10}$	6.603	49.6475	49.3597	49.0668	6.2806	5.1921	5.2384	5.5205
$\widehat{p}_{11}$	155.2	399.9443	422.7023	421.5437	149.999	149.8901	150.0354	154.4826
$\widehat{p}_{12}$	0.0498	0.3937	0.4592	0.5064	0.0577	0.0516	0.05	0.0498
$\widehat{p}_{13}$	752.9	999.9688	1020.6	1016.1	760.867	759.2227	711.8321	724.5906
$\widehat{p}_{14}$	13.51	49.2998	43.0861	45.9953	10.6713	10.28	11.5074	11.715
$\widehat{p}_{15}$	703.6	2000	1816.6	1937.2	684.614	684.5661	685.6799	700.3178
$\widehat{p}_{16}$	6056	5000	5034.2	4994.2	5999.7	5999.6	6002.2	6001.6
$\widehat{p}_{17}$	27.12	199.7554	241.1454	243.94	27.5014	26.5309	27.4755	27.3444
$\widehat{p}_{18}$	4475	4000	3934.2	3907	3666.6	3666.6	3898	4089.5
$\widehat{p}_{19}$	0.1562	2.4398	4.756	4.1083	0.4963	0.2482	0.217	0.2731
$\widehat{p}_{20}$	24.37	199.6888	330.0194	327.6911	33.07	31.6387	26.9885	27.362
$\widehat{p}_{21}$	0.0745	0.1027	0.2168	0.3136	0.06546	0.0526	0.0681	0.0673

TABLE 2. Absolute percentage error in estimated parameters.

	Technique 1: $S = 50$ and $R = 50$			Technique 2	Technique 3: $S = 10$ and $R = 10$		
Parameters	(T1-I) *fmincon*	(T1-II) PSO	(T1-III) Hybrid PSO	(T2) APE	(T3-I) APE with *fmincon*	(T3-II) APE with PSO	(T3-III) APE with Hybrid PSO
$\widehat{p}_7$	2889.31	2959.73	2923.75	73.16	45.60	33.07	40.84
$\widehat{p}_8$	70.98	80.76	74.67	2.95	2.19	0.49	0.31
$\widehat{p}_9$	796.98	937.27	977.32	18.23	8.80	1.95	3.02
$\widehat{p}_{10}$	651.89	647.53	643.10	4.88	21.37	20.67	16.39
$\widehat{p}_{11}$	157.70	172.36	171.61	3.35	3.42	3.33	0.46
$\widehat{p}_{12}$	689.93	821.35	916.05	15.77	3.53	0.32	0.08
$\widehat{p}_{13}$	32.82	35.56	34.96	1.06	0.84	5.45	3.76
$\widehat{p}_{14}$	264.91	218.92	240.45	21.01	23.91	14.82	13.29
$\widehat{p}_{15}$	184.25	158.19	175.33	2.70	2.71	2.55	0.47
$\widehat{p}_{16}$	17.44	16.87	17.53	0.93	0.93	0.89	0.90
$\widehat{p}_{17}$	636.56	789.18	799.48	1.41	2.17	1.31	0.83
$\widehat{p}_{18}$	10.61	12.08	12.69	18.06	18.06	12.89	8.61
$\widehat{p}_{19}$	1461.97	2944.81	2530.15	217.73	58.90	38.92	74.84
$\widehat{p}_{20}$	719.40	1254.20	1244.65	35.70	29.83	10.74	12.28
$\widehat{p}_{21}$	37.93	191.16	321.17	12.09	29.36	8.54	9.62

Whereas, Table-2 shows the estimation error of each parameter with respect to the benchmark parameters obtained from Chen and Mora's work [5]. The results in Table-1 and Table-2 show that the battery parameters obtained using the proposed two-stage parameters estimation methodology (T3) are more accurate compared to the parameters that are obtained either by using the optimization technique (T1) alone or by using the APE (T2) alone.

The battery parameters obtained using APE with *fmincon* (T3-I) are more accurate as compared to the ones that are obtained by using optimization techniques (T1) alone and are somewhat comparable with the ones that are obtained by using APE (T2) alone. However, the parameters obtained by the proposed technique T3-II and T3-III i.e. APE in combination with PSO and Hybrid PSO respectively are more accurate and have much lesser error with reference to the Chen and Mora's benchmark parameters values. In purely optimization based technique (T1), the number of iterations are $R = 50$ and the swarm size of $S = 50$ are selected. However, the parameters estimation error in Table-2 suggests that it requires more population of particles, and more number of iterations to give reasonable estimates of battery model parameters.

Table-1 and 2 show that the parameters estimated by the optimization technique (T1) alone have a larger error. Therefore, the following discussion will only focus on APE (T2)

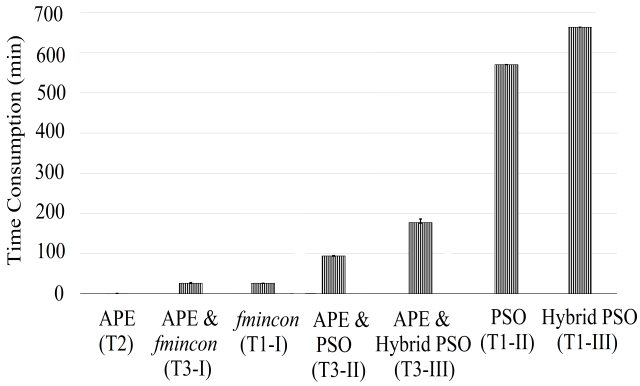

FIGURE 6. Comparison of time consumed by parameters estimation strategies.

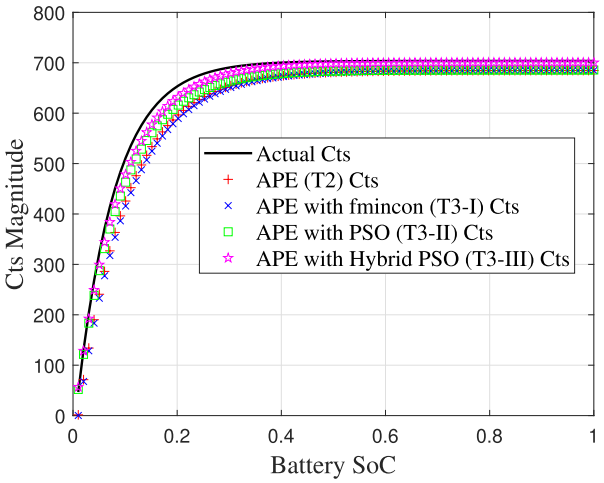

FIGURE 7. Comparison and variation of circuit element Cts for technique 2 (T2) and technique 3 (T3).

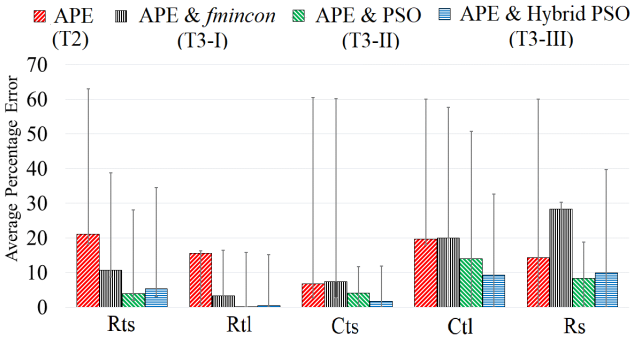

FIGURE 8. Circuit elements error analysis for technique 2 (T2) and technique 3 (T3).

and our proposed technique (T3). Table-1 shows a good match between the parameters obtained by the proposed technique (T3-II and T3-III), and the Chen and Mora's parameters values. We further evaluate the parameters estimation accuracy by calculating the battery equivalent circuit elements and estimating the battery terminal voltage. The equivalent circuit element values and estimated battery terminal voltage are compared with the ones given by Chen and Mora.

We also record the average simulation time (over 10 simulations of each technique), required by the three proposed techniques, i.e. T3-I, T3-II, and T3-III. These results are shown in Fig. 6. It can be seen from Fig. 6 that APE with PSO (T3-II), and APE with Hybrid PSO (T3-III) which give the best estimation of battery parameters have relatively larger time consumption when compared to APE (T2), APE with *fmincon* (T3-I), and the *fmincon* optimization technique (T1-I). However, the time consumption of APE with PSO (T3-II) and APE with Hybrid PSO (T3-III) is much less than the PSO (T1-II) and Hybrid PSO optimization (T1-III) techniques.

Since the accuracy of the estimated parameters using optimization techniques alone is very poor. Therefore, there will be no further assessment of optimization based technique (T1). The rest of the simulation and implementation work will focus on Technique 2 and Technique 3.

B. BATTERY CIRCUIT ELEMENTS (R_{ts}, R_{tl}, C_{ts}, C_{tl}, R_s) ESTIMATION COMPARISON

In this section, the battery is subjected to 0.5 amperes constant resistive load discharging and parameters $\widehat{p}_7, \ldots, \widehat{p}_{21}$ are estimated. These parameters are then used to calculate the battery circuit elements R_{ts}, R_{tl}, C_{ts}, C_{tl}, and R_s. As a sample, the variation of one circuit element C_{ts} with respect to battery SoC is illustrated in Fig. 7. The accuracy of rest of the circuit elements is evaluated by comparing the error between the estimated circuit elements and reference values of Chen and Mora's circuit elements. The circuit elements error analysis, using the APE technique (T2) alone and the proposed techniques T3-I, T3-II, and T3-III, is shown in Fig. 8.

The estimation error percentage, during the course of simulation, for each circuit element is obtained by subtracting the Chen and Mora's circuit element value at a particular time instant, from the ones that are obtained either via technique T2 or T3 at the same time instant, and then dividing by the Chen and Mora's circuit element value at that instant. The absolute value of this estimation error for each circuit element is recorded over time during simulation and stored in arrays. The mean of each such estimation error array gives the average percentage error in a circuit element's estimation. Overall Fig. 8 shows that APE with PSO (T3-II) and APE with Hybrid PSO (T3-III) have lesser circuit elements estimation error compared to APE alone (T2) and APE with *fmincon* (T3-I) technique. Also, the computation time required by APE with PSO (T3-II) or APE with Hybrid PSO (T3-III) is intermediate between T1-I, T2, and T3-I techniques and T1-II, and T1-III techniques as shown in Fig. 6.

C. BATTERY TERMINAL VOLTAGE ESTIMATION COMPARISON

The battery terminal voltage is estimated using four different load profiles with irregular discharging intervals. These load

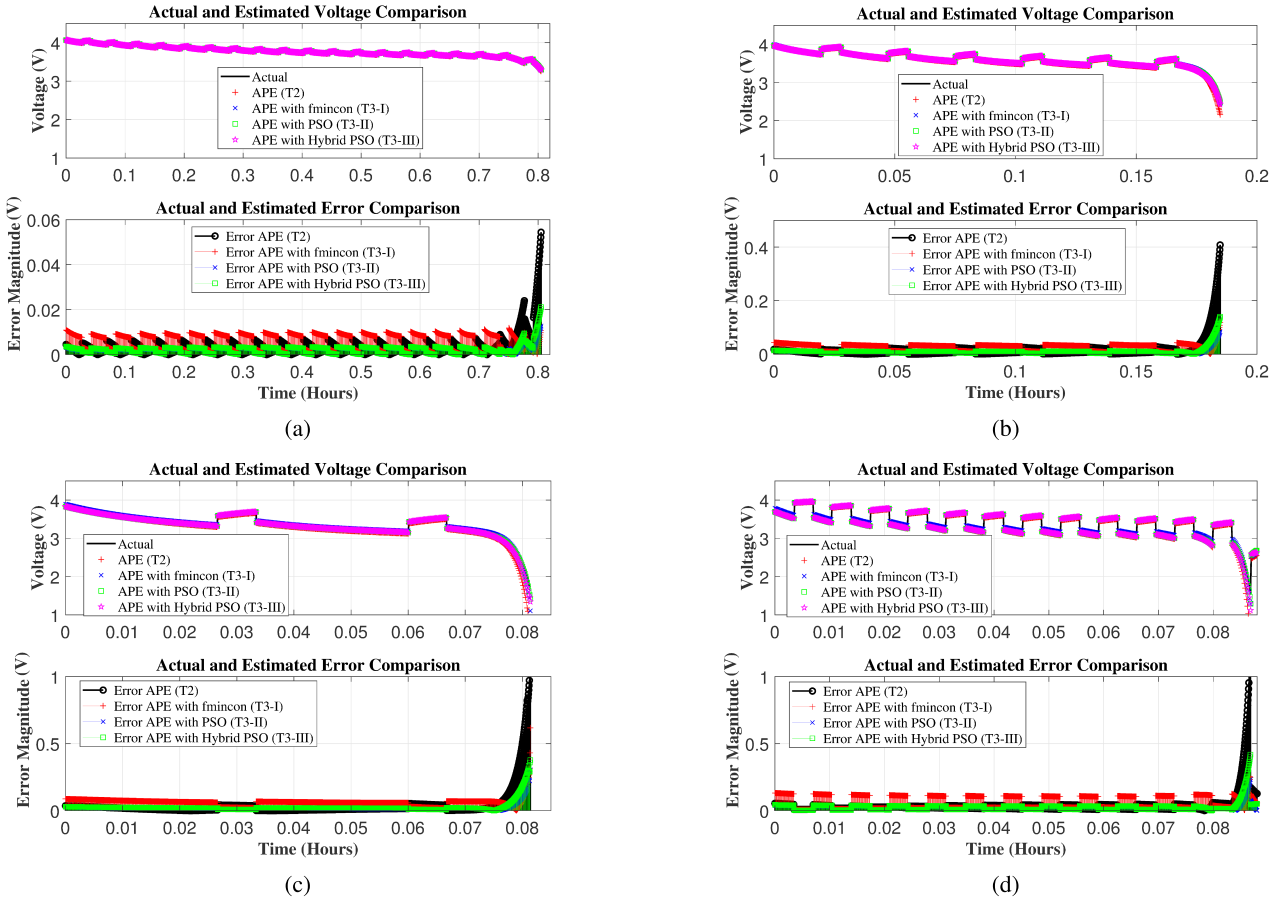

FIGURE 9. Terminal voltage estimation and absolute error $|e(t)|$ comparison among Chen and Mora, technique 2 (T2) and technique 3 (T3) for four load profiles. (a) Terminal voltage estimation and absolute error $|e(t)|$ calculation for load profile 1. (b) Terminal voltage estimation and absolute error $|e(t)|$ calculation for load profile 2. (c) Terminal voltage estimation and absolute error $|e(t)|$ calculation for load profile 3. (d) Terminal voltage estimation and absolute error $|e(t)|$ calculation for load profile 4.

TABLE 3. Battery discharging load profiles.

Load profiles	Current Magnitude A	Time Period seconds	OFF Time seconds	ON Time seconds
Load Profile 1	0.5	150	52.5	97.5
Load Profile 2	2	100	30	70
Load Profile 3	4	120	24	96
Load Profile 4	6	25	12.5	12.5

profiles are given in Table-3. The battery current in these load profiles varies from 0.5 amperes to 6 amperes while the total simulation time period changes from 150 seconds to 25 seconds as shown in Table-3. For all the four load profiles, the battery is discharged until the SoC reaches 7%.

The results of battery terminal voltage estimation and their respective estimation error for the four designed load profiles are illustrated in Fig. 9a to Fig. 9d. The zoomed in views of terminal voltage estimation error of Technique 2 (T2) and Technique 3 (T3), for four load profiles are also shown in Fig. 10. Note that the absolute value of terminal voltage estimation error is shown in Fig. 9 and Fig. 10.

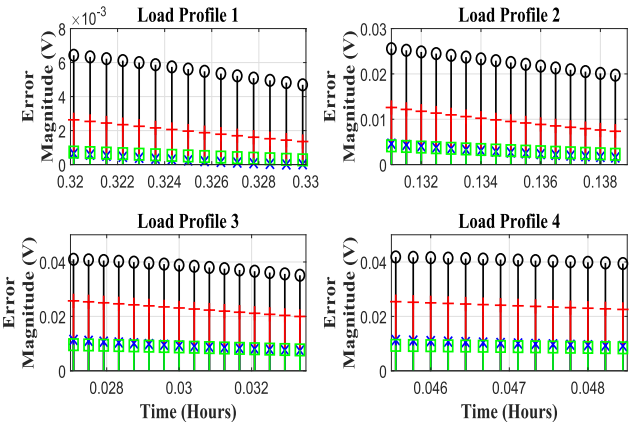

FIGURE 10. Zoomed in view of terminal voltage estimation error for technique 2 (T2) and technique 3 (T3), for four load profiles (data labels same as $|e(t)|$ plots in Fig. 9).

The voltage estimated by using Chen and Mora's parameters values, is termed as actual voltage in Fig. 9. The voltage estimation error is obtained by subtracting the voltage estimated by Technique 2 or 3 from Chen and Mora's voltage.

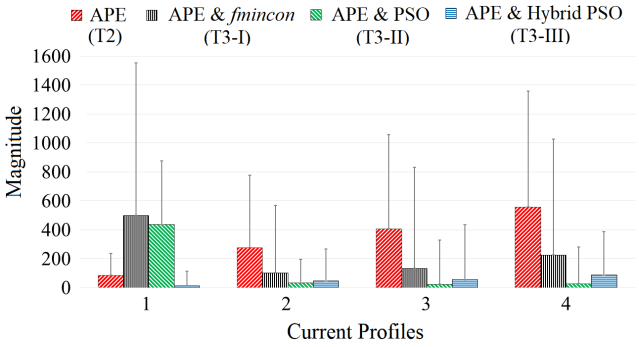

FIGURE 11. $\sum_{t=t_0}^{T} e^2(t)$ **Analysis for technique 2 (T2) and technique 3 (T3) for four load profiles.**

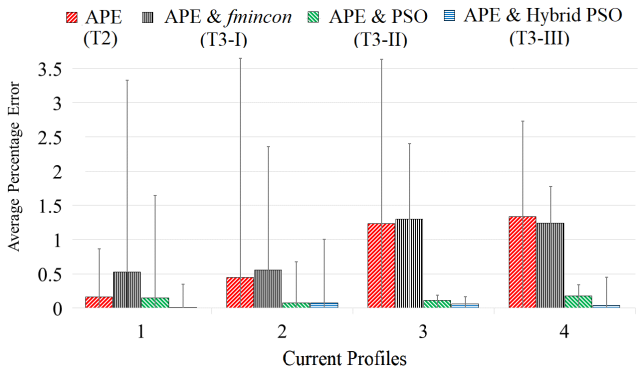

FIGURE 12. **Average of absolute terminal voltage error for technique 2 (T2) and technique 3 (T3) for four load profiles.**

The terminal voltage estimation error is reduced using the battery parameters obtained from APE with PSO (T3-II) and APE with Hybrid PSO (T3-III), especially in the relaxation period when the battery is not discharging and when SoC becomes less than 10%.

For the discharging current profiles defined in Table-3, the quantity $\sum_{t=t_0}^{T} e^2(t)$, and average of absolute percentage error of terminal voltages, estimated using techniques T2 and T3, are also highlighted in Fig. 11 and Fig. 12 respectively. The time duration for the terminal voltage error analysis is $t = [t_0, T]$, where T is the time at which the battery SoC approaches to 7%. The overall results in these figures, for the four designed discharging load profiles show that the quantity $\sum_{t=t_0}^{T} e^2(t)$, and average of absolute terminal voltage error for APE (T2) and APE with *fmincon* (T3-I) are larger than APE with PSO (T3-II), and APE with Hybrid PSO (T3-III).

The only anomaly in these computer simulations is that APE with PSO (T3-II) has a higher value for the quantity $\sum_{t=t_0}^{T} e^2(t)$, when the discharging load profile 1 is used, i.e. the battery is discharged with a low current and larger time period. This anomaly is further evaluated in our experimental investigation.

Our simulation results for parameters estimation, battery circuit elements calculation and battery terminal voltage estimation show that proposed two-stage methodology consisting of APE with PSO (T3-II) and APE with Hybrid PSO (T3-III) perform better than the purely optimization based techniques (T1), APE (T2) and APE with *fmincon* (T3-I) techniques. Moreover, the proposed APE with PSO (T3-II), and APE with Hybrid PSO (T3-III) techniques need less computation time compared to purely optimization based techniques (T1-II), and (T1-III) to estimate battery model parameters more accurately.

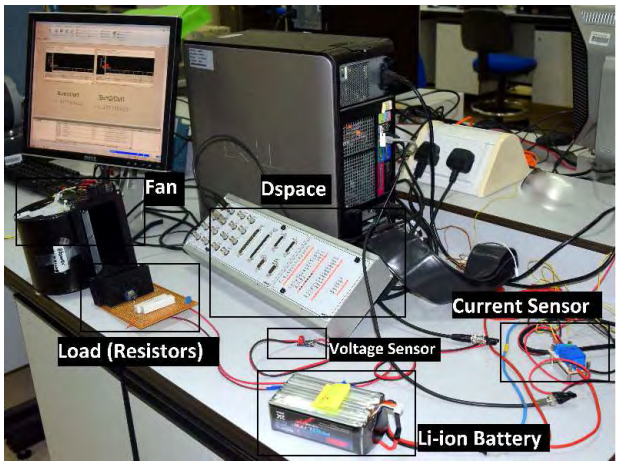

FIGURE 13. **Experimental setup.**

V. EXPERIMENTAL VALIDATION OF THE PROPOSED TECHNIQUE

The simulation results showed very poor accuracy of the estimated parameters $\widehat{p}_7, \ldots, \widehat{p}_{21}$ when using purely optimization based technique (T1). Therefore, only Technique 2 and our proposed Technique 3 will be experimentally investigated for the accuracy assessment of the estimated parameters. The experimental setup designed for this work is shown in Fig. 13. This setup, similar to [1] includes a Thunder-Power 22.2 V, 6.6 Ah Lithium-Polymer battery ($TP6600-6SP+25$), different type of loads for battery discharging, voltage and current sensors for the battery voltage and current measurements. A dSPACE 1103 board is used for experimentation and data acquisition. A sampling period of 0.01 seconds is selected to measure the voltage and current of a Lithium-Polymer battery.

The voltage relaxation test is performed to get the open circuit voltage curve as a function of battery SoC. Curve fitting, as mentioned in the background section (II.A), is used to get the open circuit voltage parameters $\widehat{p}_1, \ldots, \widehat{p}_6$ of equation (5). The values obtained for these parameters are; $p_1 = 5.112, p_2 = 40.955, p_3 = 22.195, p_4 = 1.9215, p_5 = 1.759, p_6 = 3.0435$, which are the same as shared in our earlier work [1]. The major focus of this work is estimation and accuracy assessment of the remaining battery parameters $\widehat{p}_7, \ldots, \widehat{p}_{21}$.

Subsection V.A presents the experimental estimation of the battery model parameters $\widehat{p}_7, \ldots, \widehat{p}_{21}$. Subsection V.B assess

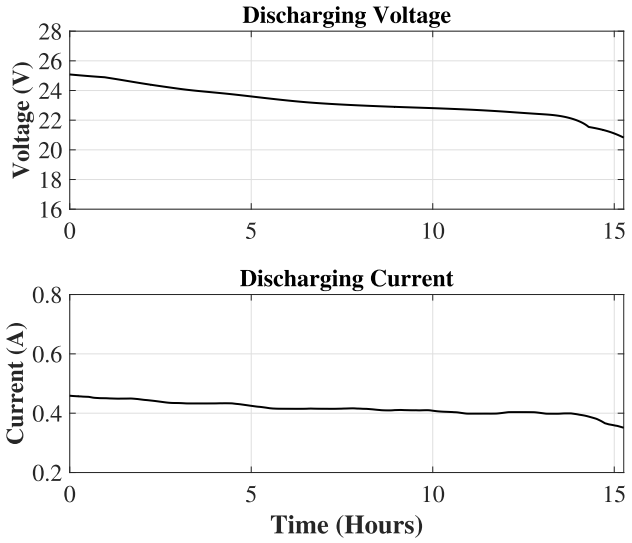

FIGURE 14. Discharging voltage and current profiles of Lithium-Polymer battery connected with 50 Ω resistor.

TABLE 4. Experimental parameters estimation of 22.2 V, 6.6 Ah Lithium Polymer battery.

	Technique 2	Technique 3: $S = 10$ and $R = 10$		
Parameters	(T2) APE values	(T3-I) APE with *fmincon*	(T3-II) APE with PSO	(T3-III) APE with Hybrid PSO
$\widehat{p}_7$	0.5505	0.5493	0.5525	0.5436
$\widehat{p}_8$	30.0475	29.9866	30.0538	29.7022
$\widehat{p}_9$	0.0551	0.0549	0.0536	0.0538
$\widehat{p}_{10}$	6.2585	6.0380	6.2454	5.9850
$\widehat{p}_{11}$	30	29.8603	30.0176	29.5146
$\widehat{p}_{12}$	0.0551	0.0549	0.0545	0.0536
$\widehat{p}_{13}$	760.2266	760.2144	754.6998	754.6072
$\widehat{p}_{14}$	10.7686	10.0683	10.0012	9.3990
$\widehat{p}_{15}$	685.7457	685.7182	674.5923	674.6247
$\widehat{p}_{16}$	6036.4	6036.7	5991.9	5995.3
$\widehat{p}_{17}$	27.5422	27.2466	27.4837	26.8348
$\widehat{p}_{18}$	3696	3696	3649.5	3650
$\widehat{p}_{19}$	0.0439	0.0449	0.0450	0.0447
$\widehat{p}_{20}$	59.07	58.8419	60.0453	58.8088
$\widehat{p}_{21}$	0.2246	0.2078	0.1186	0.1527

the accuracy of estimated battery parameters by comparing the estimated and measured voltage for sixteen discharging load profiles. Finally, subsection V.C evaluates the parameters estimation accuracy again by comparing the estimated and measured voltage for charging process of sixteen individual batteries.

A. EXPERIMENTAL ESTIMATION OF BATTERY MODEL PARAMETERS

In this section, the battery model parameters $\widehat{p}_7, \ldots, \widehat{p}_{21}$ are estimated using the APE (T2) and our proposed two-stage parameters estimation technique (T3). A fully charged Lithium-Polymer battery is connected with the 50 Ω resistive load, to discharge the battery with a small load current of about 0.4 amperes. The slow battery discharging during APE process ensures the convergence of product of estimated resistances and capacitances to the product of actual resistances and capacitances, as proved in our earlier work [1]. Therefore, it provides accurate estimates of battery model circuit elements $R_{ts}, R_{tl}, C_{ts}, C_{tl}$, and R_s which will ensure an accurate estimation of battery terminal voltage. The battery terminal voltage and discharging current profiles are shown in Fig. 14. It took about 15 hours to discharge the battery upto 7% of its rated capacity with a load resistance of 50 Ω. The voltage and current data used for parameter estimation contains 5,493,994 number of samples each, and are utilized in Algorithm 1 to estimate Lithium-Polymer battery parameters. Algorithm 1 is the combination of the APE algorithm (Lines 1 to 16) and optimization algorithm (Lines 17 to 29). The APE algorithm, detailed in section (II.B), uses UAS, the adaptive equation (19), and curve fitting to estimate the Lithium-Polymer battery parameters. The estimated parameters, using APE technique (T2), are recorded in column 2 of Table-4.

Next, the parameters obtained by the APE technique (T2) are utilized to choose the search space (intervals) of parameters $\widehat{p}_7, \ldots, \widehat{p}_{21}$, for further optimization. The parameters obtained by APE (T2) are optimized in the second stage of Algorithm 1. The search space interval of the optimization techniques (T3-I) to (T3-III), for each parameter is designed by setting the upper and lower bounds, δ_n. Similar to the simulation setup, for experimental verification, the value of δ_n is set at 10 percent of the value of parameters estimated by the APE process, i.e. $\delta_n = 0.1\widehat{p}_n$ and $n \in \{7, \cdots, 21\}$. Thus the search space interval of the estimated parameters are defined as $\widehat{p}_7 \pm \delta_7, \ldots, \widehat{p}_{21} \pm \delta_{21}$. Furthermore, at the second stage of the proposed technique (T3), the number of iterations $R = 10$ for (T3-I) to (T3-III), and a swarm size of $S = 10$ is used for (T3-II) and (T3-III). The estimated parameters using APE with *fmincon* (T3-I), APE with Particle Swarm Optimization (T3-II), and APE with Hybrid PSO (T3-III) are tabulated in columns 3, 4, and 5 of Table-4 respectively. The optimization techniques are employed to improve the accuracy of the parameters that are originally obtained by using APE (T2). The estimated parameters accuracy is assessed in the following subsections V.B and V.C.

B. PARAMETERS ESTIMATION ACCURACY ASSESSMENT VIA BATTERY DISCHARGING TESTS

This section evaluates the accuracy of the estimated parameters obtained by APE (T2) and our proposed technique (T3) via battery discharging. The estimated parameters are used to calculate the values of battery circuit elements $R_{ts}, R_{tl}, C_{ts}, C_{tl}, R_s$ which are then used to estimate the battery terminal voltage. Thus, the accuracy of estimated parameters is evaluated by comparing the estimated and measured battery voltage. The 22.2 V, 6.6 Ah Lithium-Polymer battery is connected with resistive load and the battery is discharged until the SoC approaches 7%. Sixteen different rigorous load profiles are designed for battery discharging and data

i.e. estimated and measured terminal voltages are acquired. These sixteen discharging load profiles are separated in the form of five groups. Group 1 discharges the battery through a constant load resistance, Group 2 discharges the battery with the periodic ON and OFF intervals while Groups 3 to 5 discharge the battery with random ON and OFF intervals. The details of these sixteen discharging load profiles are given below.

- Group 1 (G1), 4 Tests: The battery is subjected to discharge through a constant resistive load, using one of the following four resistive loads of 50 Ω, 25 Ω, 11.11 Ω and 7.5 Ω.
- Group 2 (G2), 4 Tests: In this group the battery is periodically discharged and relaxed with different loads. The four load profiles designed in this group are:
  - The battery is discharged for 15 minutes followed by relaxation time of 15 minutes using two load resistors, 25 Ω and 11.11 Ω.
  - The battery is discharged for 1 minute followed by relaxation time of 1 minute using two load resistors, 25 Ω and 11.11 Ω.
- Group 3 (G3), 3 Tests: The discharging tests in this group are conducted with randomly varying ON and OFF times, in contrast to Group 2 which has periodic ON and OFF times. The experiments are performed with three values of resistive loads, i.e. 25 Ω, 11.11 Ω and 7.5 Ω.
- Group 4 (G4), 2 Tests: These tests are also performed with randomly varying ON and OFF time using light bulbs as a load. The following two load profiles are designed.
  - Parallel combination of two 24 V, 60 W DC bulbs
  - Parallel combination of three 24 V, 60 W DC bulbs
- Group 5 (G5), 3 Tests: This group contains the last three load profiles of our rigorous testing. The tests are again conducted with randomly varying ON and OFF time. Three load profiles are designed using parallel combination of three 24 V, 60 W DC bulbs. The number of bulbs in parallel combination is randomly varied from one bulb to three bulbs.

1) DISCHARGING TESTS RESULTS AND DISCUSSION

The Lithium-Polymer battery is discharged under the aforementioned 16 load profiles that are separated in five groups. The terminal voltage estimation errors, for all the sixteen discharging load profiles, are recorded in an array, for APE technique (T2) and for the developed two-stage technique (T3). As a sample, the estimated and measured terminal voltage along with the absolute voltage estimation error for two of the sixteen discharging load profiles are shown in Fig. 15 and Fig. 17. The zoomed in views of terminal voltage estimation error in Fig. 15 and Fig. 17 are also provided in Fig. 16 and Fig. 18 respectively. Figure 15 shows that voltage error profiles of APE (T2) and APE with *fmincon* (T3-I) techniques are about the same. However, APE with PSO

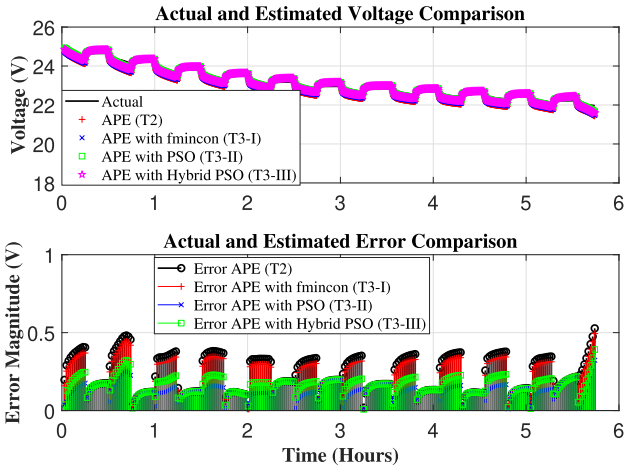

FIGURE 15. Terminal voltage estimation and absolute error $|e(t)|$ comparison for resistive load of 11.11 Ω with 15 minutes ON and 15 minutes OFF times.

FIGURE 16. Zoomed in view of terminal voltage error comparison for resistive load of 11.11 Ω with 15 minutes ON, and 15 minutes OFF times (data labels same as $|e(t)|$ plots in Fig. 15).

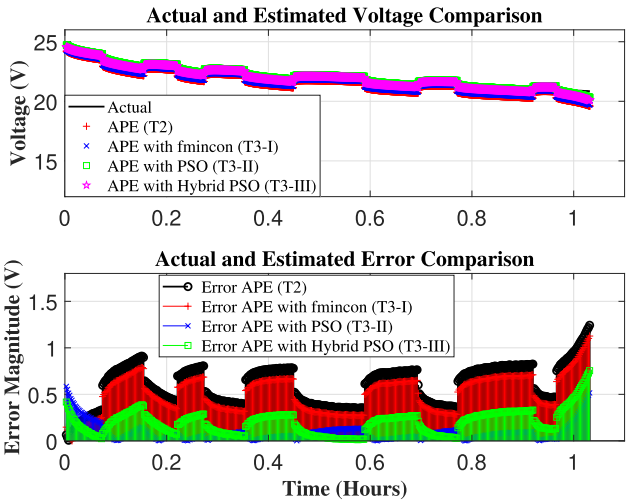

FIGURE 17. Terminal voltage estimation and absolute error $|e(t)|$ comparison for randomly varying load with random ON and OFF times drawing 5 A and 7.5 A.

(T3-II) and APE with Hybrid PSO (T3-III) show a significant drop in the voltage estimation error magnitude. In Fig. 17, the voltage estimation error is investigated

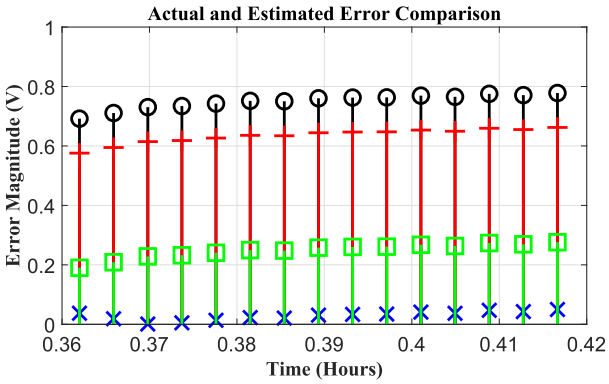

FIGURE 18. Zoomed in view of terminal voltage error comparison for randomly varying load with random ON and OFF times drawing 5 A and 7.5 A (data labels same as $|e(t)|$ plots in Fig. 17).

TABLE 5. Terminal voltage estimation error statistics while discharging the battery with sixteen different load profiles for technique 2 (T2) and technique 3 (T3).

Parameters Estimation Methods	Mean	Median	Mode	Standard Deviation
APE (T2)	0.0211	0.027	-0.055	0.5026
APE with fmincon (T3-I)	0.0022	0.0234	-0.083	0.489
APE with PSO (T3-II)	-0.0973	-0.0252	0.0278	0.4316
APE with Hybrid PSO (T3-III)	-0.0604	-0.0023	0.138	0.4496

when the battery is subjected to a random and relatively higher discharging current. A significant reduction in error profile magnitude is noticed in Fig. 17 when APE with PSO (T3-II) and APE with Hybrid PSO (T3-III) techniques are employed. Thus, the reduction in the terminal voltage estimation error for (T3-II) and (T3-III) techniques verifies the accuracy of the estimated parameters.

Sixteen terminal voltage estimation error arrays are obtained from sixteen discharging load profiles. Due to the different discharging interval of each load profile, each array has different number of samples. To perform the overall error analysis, all the sixteen terminal voltage estimation error arrays are stacked to form a large array. Such four large terminal voltage estimation error arrays, i.e. one array for technique T2 and one for each of the techniques T3-I, T3-II and T3-III, are formed. The total number of samples, in each large terminal voltage estimation error array, is 2.75×10^7. The mean, median, mode and standard deviation for each of these four terminal voltage estimation error arrays are described in Table-5. An extensive investigation of the overall terminal voltage estimation error arrays is carried out by further showing their histogram and cumulative distribution graphs in Fig. 19 and Fig. 20 respectively. Where, the red vertical lines in Fig. 20 indicate the $\pm 4.5\%$ terminal voltage estimation error i.e. ± 1 V. The following observations can be made from the data presented in Table-5, Fig. 19 and Fig. 20.

- In Table-5, the standard deviation values imply that the terminal voltage estimation error is less dispersed and settled around the small mode value for APE with PSO (T3-II) and APE with Hybrid PSO (T3-III) techniques.
- Fig. 19 shows that for more than 95% of the samples, the terminal voltage error lies within ± 1 V for T2 and all T3 techniques. Also, the low standard deviation of terminal voltage estimation error, settled around mode value, for T3-II and T3-III techniques can be seen from the histogram in Fig. 19.
- Fig. 20 shows that the percentage of samples for which the voltage estimation error lies within ± 1 V ($\pm 4.5\%$ range) is: 95.43% for APE (T2), 95.78% for APE with *fmincon* (T3-I), 97.29% for APE with PSO (T3-II), and 97.08% for APE with Hybrid PSO (T3-III). Furthermore, the percentage of samples for which the voltage estimation error lies within ± 0.5 V ($\pm 2.25\%$ range) is: 86.90% for APE (T2), 87.33% for APE with *fmincon*

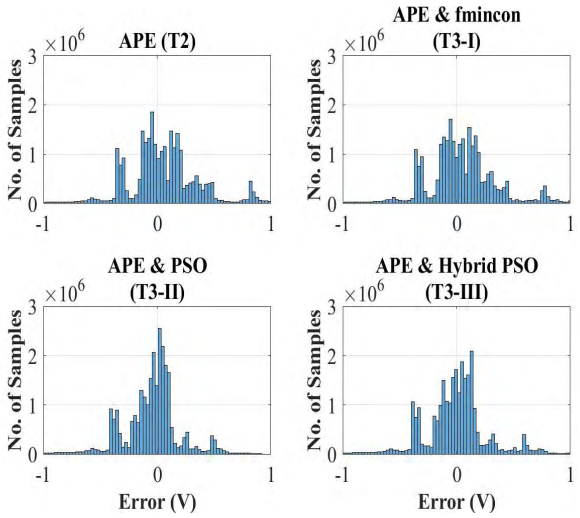

FIGURE 19. Histogram of terminal voltage estimation error for technique 2 (T2) and technique 3 (T3) under sixteen different discharging profiles.

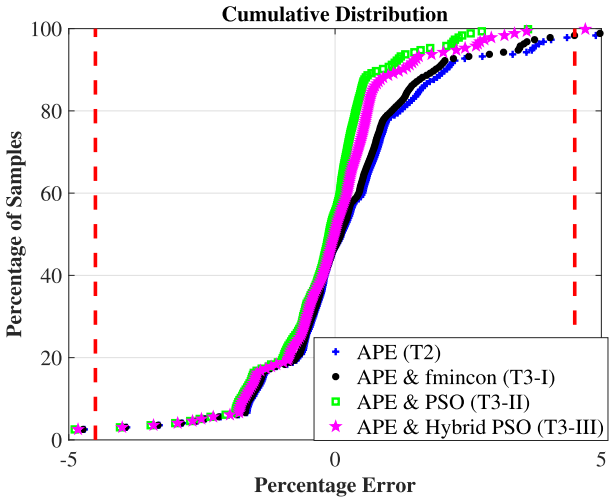

FIGURE 20. Cumulative distribution of terminal voltage estimation error for techique 2 (T2) and technique (T3) under sixteen different discharging profiles.

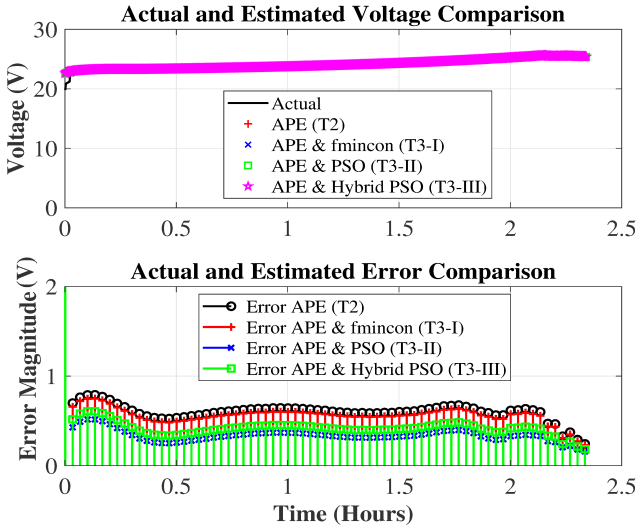

FIGURE 21. Terminal voltage estimation and absolute error $|e(t)|$ comparison while charging the 22.2 V, 6.6 Ah Li-Polymer battery, technique 2 (T2) and technique 3 (T3).

(T3-I), 91.74% for APE with PSO (T3-II), and 89.12% for APE with Hybrid PSO (T3-III).

Thus the statistical analysis presented in Table-5, Fig. 19 and Fig. 20 for battery discharging shows that battery parameters estimated using APE with PSO (T3-II) and APE with Hybrid PSO (T3-III) are more accurate as compared to APE (T2) and APE with *fmincon* (T3-I) techniques.

C. PARAMETERS ESTIMATION ACCURACY ASSESSMENT VIA BATTERY CHARGING TESTS

In this section, we present results related to charging sixteen individual batteries with a constant current of 2.5 amperes using the Thunder-Power charger (TP820CD). The estimated and measured voltage of the battery using Technique 2 and Technique 3 are compared to assess the accuracy of the estimated battery parameters. The voltage estimation error is recorded for each battery during the charging process. As a sample, detailed data collected for one battery during the charging process is shown in Fig. 21. The zoomed in view of terminal voltage estimation error in Fig. 21, is also shown in Fig. 22. The error magnitude plot shows that APE (T2) and APE with *fmincon* (T3-I) techniques have higher terminal voltage estimation errors compared to APE with PSO (T3-II) and APE with Hybrid PSO (T3-III) techniques.

For all the sixteen batteries, four terminal voltage estimation error arrays using T2, T3-I, T3-II, T3-III techniques, similar to the battery discharging case, are formed. Each array includes the terminal voltage estimation error of all the sixteen individual batteries. The total number of samples collected in each array during the batteries charging are 1.258×10^7. The statistical error analysis of these four error arrays is provided in Table-6. The terminal voltage estimation error, of all the sixteen individual batteries, is further analyzed

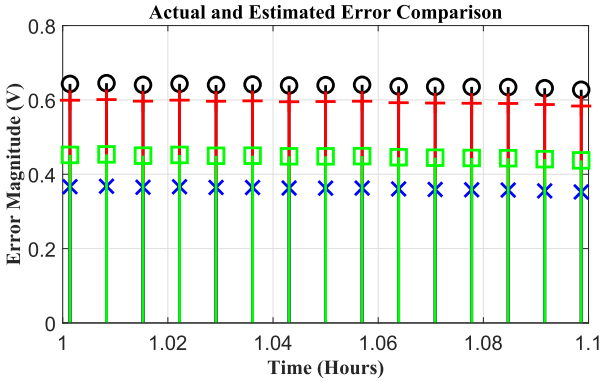

FIGURE 22. Zoomed in view of terminal voltage error comparison while charging the 22.2 V, 6.6 Ah Li-Polymer battery, technique 2 (T2) and technique 3 (T3) (data labels same as $|e(t)|$ plots in Fig. 21).

TABLE 6. Terminal voltage estimation error statistics while charging sixteen different batteries with a constant 2.5 A for technique 2 (T2) and technique 3 (T3).

Parameters Estimation Methods	Mean	Median	Mode	Standard Deviation
APE (T2)	-0.6509	-0.6396	-0.641	0.3847
APE with fmincon (T3-I)	-0.6110	-0.5969	-0.589	0.3828
APE with PSO (T3-II)	-0.3879	-0.3699	-0.308	0.3787
APE with Hybrid PSO (T3-III)	-0.4723	-0.4538	-0.4895	0.3824

by performing the histogram analysis, and cumulative distribution analysis as shown in Fig. 23 and Fig. 24 respectively. The data presented in Table-6, Fig. 23 and Fig. 24 can be analyzed as follows:

- Table-6 shows that mean, median, mode and standard deviation values for APE with PSO (T3-II) and APE with Hybrid PSO (T3-III) are relatively lower than APE (T2) and APE with *fmincon* (T3-I) techniques.
- Figure 23 shows that for more than 94% of samples, the terminal voltage estimation error lies within ± 1 V for T2 and all T3 techniques. Also, the terminal voltage estimation error is less dispersed and settled around a small mode value, for T3-II and T3-III techniques.
- Figure 24 shows that the percentage of samples for which the voltage estimation error lies within ± 1 V ($\pm 4.5\%$ range) is: 94.34% for APE (T2), 95.55% for APE with *fmincon* (T3-I), 99.35% for APE with PSO (T3-II), and 98.26% for APE with Hybrid PSO (T3-III). Furthermore, the percentage of samples for which the voltage estimation error data that lies within ± 0.6 V (2.7% range) for different techniques is: 38.32% for APE (T2), 50.72% for APE with *fmincon* (T3-I), 89.01% for APE with PSO (T3-II), and 81.98% for APE with Hybrid PSO (T3-III).

The study of terminal voltage estimation error while charging sixteen individual batteries with a constant 2.5 amperes current shows that the proposed APE with PSO (T3-II) and APE with Hybrid PSO (T3-III) techniques estimate the battery model parameters more accurately compared

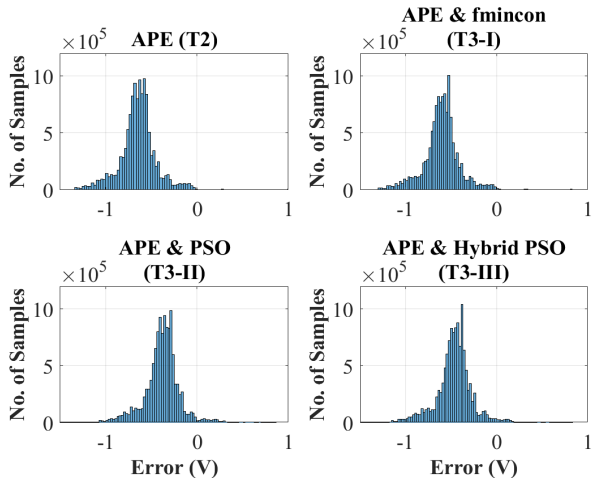

FIGURE 23. Histogram of terminal voltage estimation error for technique 2 (T2) and technique 3 (T3) while charging sixteen individual batteries with a constant 2.5 A current.

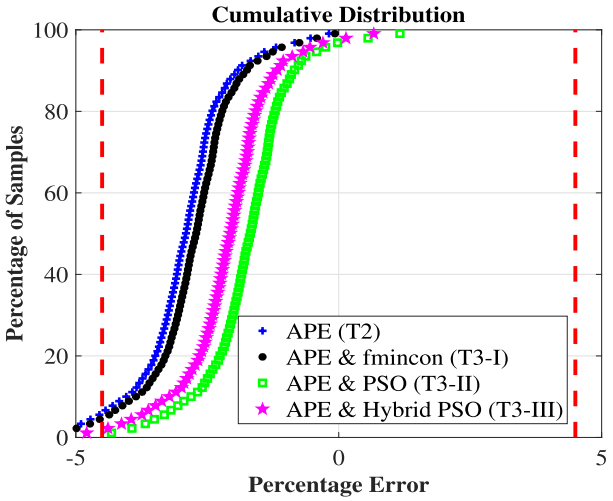

FIGURE 24. Cumulative distribution of terminal voltage estimation error for technique 2 (T2) and technique 3 (T3) While charging sixteen individual batteries with a constant 2.5 A current.

to APE (T2) and optimization techniques (T1) alone.

VI. CONCLUSION

This paper demonstrated the effectiveness of our proposed two-stage technique for accurate estimation of Li-ion battery parameters. At the first stage, the initial estimates of parameters values are obtained by using an adaptive parameters estimation (APE) technique. The APE helps in finding these initial estimates, which help to narrow the search space (intervals) used in the second stage of the proposed technique, for further refinement of the initially estimated parameters values. The narrowed search space (interval) when used with an optimization routine, requires less computational time, compared to an unguided or arbitrarily initialized optimization routine. As the second stage of the proposed technique, Particle Swarm, and Hybrid Particle Swarm Optimization routines were observed to further improve the accuracy of the initial parameters obtained by APE.

The estimated battery parameters values are utilized to estimate the Li-ion battery circuit elements, and battery terminal voltage, both in rigorous simulation and rigorous experimental investigation. The simulation study compares the estimated parameters and circuit elements values, to results available in the literature. In the experimental study, the effectiveness of the proposed technique is evaluated by comparing the estimated and the actual voltage measured across the battery terminals, and by further performing a statistical analysis. Both the simulation and experimental investigations show the effectiveness of the proposed two-stage UAS based optimization technique for Li-ion battery model parameters estimation.

REFERENCES

[1] D. Ali, S. Mukhopadhyay, H. Rehman, and A. Khurram, "UAS based Li-Ion battery model parameters estimation," *Control Eng. Pract.*, vol. 66, pp. 126–145, Sep. 2017.

[2] M. A. Hannan, M. S. H. Lipu, A. Hussain, and A. Mohamed, "A review of lithium-ion battery state of charge estimation and management system in electric vehicle applications: Challenges and recommendations," *Renew. Sustain. Energy Rev.*, vol. 78, pp. 834–854, Oct. 2017.

[3] S. Tang, Y. Wang, Z. Sahinoglu, T. Wada, S. Hara, and M. Krstic, "State-of-charge estimation for lithium-ion batteries via a coupled thermal-electrochemical model," in *Proc. Amer. Control Conf. (ACC)*, 2015, pp. 5871–5877.

[4] D. A. Pola *et al.*, "Particle-filtering-based discharge time prognosis for lithium-ion batteries with a statistical characterization of use profiles," *IEEE Trans. Rel.*, vol. 64, no. 2, pp. 710–720, Jun. 2015.

[5] M. Chen and G. A. Rincon-Mora, "Accurate electrical battery model capable of predicting runtime and I–V performance," *IEEE Trans. Energy Convers.*, vol. 21, no. 2, pp. 504–511, Jun. 2006.

[6] W.-J. Shen and H.-X. Li, "A sensitivity-based group-wise parameter identification algorithm for the electric model of Li-Ion battery," *IEEE Access*, vol. 5, pp. 4377–4387, 2017.

[7] Y. Wang and L. Li, "Li-Ion battery dynamics model parameter estimation using datasheets and particle swarm optimization," *Int. J. Energy Res.*, vol. 40, no. 8, pp. 1050–1061, 2016.

[8] C. S. Huang, T. W.-S. Chow, and M.-Y. Chow, "Li-Ion battery parameter identification with low pass filter for measurement noise rejection," in *Proc. 26th IEEE Int. Symp. Ind. Electron.*, Jun. 2017, pp. 2075–2080.

[9] D. Dvorak, T. Bäuml, A. Holzinger, and H. Popp, "A comprehensive algorithm for estimating lithium-ion battery parameters from measurements," *IEEE Trans. Sustain. Energy*, vol. 9, no. 2, pp. 771–779, Apr. 2017.

[10] K. Mueller, E. Schwiederik, and D. Tittel, "Analysis of parameter identification methods for electrical Li-Ion battery modelling," in *Proc. World Electr. Vehicle Symp. Exhib. (EVS)*, Nov. 2013, pp. 1–9.

[11] P. Kumar and P. Bauer, "Parameter extraction of battery models using multiobjective optimization genetic algorithms," in *Proc. 14th Int. Power Electron. Motion Control Conf. (EPE/PEMC)*, 2010, pp. 106–110.

[12] D. Kapoor, P. Sodhi, and A. Keyhani, "Estimation of parameters for battery storage models," in *Proc. IEEE Conf. Energy Convers.*, Oct. 2014, pp. 406–411.

[13] J. C. Forman, S. J. Moura, J. L. Stein, and H. K. Fathy, "Genetic identification and fisher identifiability analysis of the Doyle–Fuller–Newman model from experimental cycling of a $LiFePO_4$ cell," *J. Power Sources*, vol. 210, pp. 263–275, Jul. 2012.

[14] Z. Yu, L. Xiao, H. Li, X. Zhu, and R. Huai, "Model parameter identification for lithium batteries using the coevolutionary particle swarm optimization method," *IEEE Trans. Ind. Electron.*, vol. 64, no. 7, pp. 5690–5700, Jul. 2017.

[15] M. A. Rahman, S. Anwar, and A. Izadian, "Electrochemical model parameter identification of a lithium-ion battery using particle swarm optimization method," *J. Power Sources*, vol. 307, pp. 86–97, Mar. 2016.

[16] M. Clerc and J. Kennedy, "The particle swarm-explosion, stability, and convergence in a multidimensional complex space," *IEEE Trans. Evol. Comput.*, vol. 6, no. 1, pp. 58–73, Feb. 2002.
[17] N. Omar *et al.*, "Optimization of an advanced battery model parameter minimization tool and development of a novel electrical model for lithium-ion batteries," *Int. Trans. Elect. Energy Syst.*, vol. 24, no. 12, pp. 1747–1767, Dec. 2014.
[18] H. M. U. Butt, S. Mukhopadhyay, and H. Rehman, "A two stage, adaptive-optimized Li-Ion battery parameters estimation strategy," in *Proc. 11th Int. Symp. Mechatron. Appl. (ISMA)*, 2018, pp. 1–7.
[19] J. Kennedy and R. Eberhart, "Particle swarm optimization," in *Proc. IEEE Int. Conf. Neural Netw.*, Perth, WA, Australia, Nov./Dec. 1995, pp. 1942–1945.
[20] S. Mukhopadhyay and F. Zhang, "Adaptive detection of terminal voltage collapses for Li-Ion batteries," in *Proc. IEEE 51st Annu. Conf. Decision Control (CDC)*, Dec. 2012, pp. 4799–4804.
[21] D. Ali, S. Mukhopadhyay, and H. Rehman, "A novel adaptive technique for Li-Ion battery model parameters estimation," in *Proc. IEEE Nat. Aerosp. Electron. Conf. Ohio Innov. Summit*, Jul. 2016, pp. 23–26.
[22] A. M. Mathai and H. J. Haubold, "Mittag-Leffler functions and fractional calculus," in *Special Functions for Applied Scientists*. New York, NY, USA: Springer, 2008, pp. 79–134.
[23] S. Mukhopadhyay and F. Zhang, "A high-gain adaptive observer for detecting Li-Ion battery terminal voltage collapse," *Automatica*, vol. 50, no. 3, pp. 896–902, Mar. 2014.
[24] A. Ilchmann, *Non-Identifier-Based High-Gain Adaptive Control* (Lecture Notes in Control and Information Sciences), vol. 189. Berlin, Germany: Springer-Verlag, 1993.
[25] Y. Li and Y. Chen, "When is a Mittag–Leffler function a Nussbaum function?" *Automatica*, vol. 45, no. 8, pp. 1957–1959, 2009.
[26] S. Mukhopadhyay. Mittag-Leffler Function, M-file, cmex DLL, and S-Function. File Exchange: MATLAB Central. Accessed: Aug. 29, 2018. [Online]. Available: https://www.mathworks.com/matlabcentral/fileexchange/20731
[27] *MATLAB fmincon Optimization Toolbox*. Accessed: Aug. 29, 2018. [Online]. Available: https://www.mathworks.com/help/optim/ug/fmincon.html

HAFIZ M. USMAN received the B.Sc. degree in electrical engineering from the University of Engineering and Technology at Lahore, Lahore, Pakistan, in 2016. He is currently pursuing the M.Sc. degree in electrical engineering at the American University of Sharjah (AUS), United Arab Emirates. He has been a Research Assistant at AUS since 2016.

SHAYOK MUKHOPADHYAY received the B.E. degree in electrical engineering, from the College of Engineering Pune, Savitribai Phule Pune University (formerly known as the University of Pune), India, in 2006, the M.Sc. degree in electrical engineering from Utah State University, Logan, UT, USA, in 2009, and the Ph.D. degree in electrical engineering from the Georgia Institute of Technology, Atlanta, GA, USA, in 2014. He has been an Assistant Professor with the Department of Electrical Engineering, American University of Sharjah, United Arab Emirates (UAE), since 2014. His research interests include control, nonlinear systems, computational methods, battery modeling and failure detection, and robotic path planning. He received the Award for the Best Presentation in the Nonlinear Systems III Session from the American Control Conference 2014. He was part of a five-person team that received the national category of the UAE AI and Robotics for Good Awards for developing an In-Pipe Inspection Robot in 2017.

HABIBUR REHMAN received the B.Sc. degree in electrical engineering from the University of Engineering and Technology at Lahore, Lahore, Pakistan, in 1990, and the M.S. and Ph.D. degrees in electrical engineering from The Ohio State University, Columbus, OH, USA, in 1995 and 2001, respectively. He has a wide experience in the areas of power electronics and motor drives in both industry and academia. From 1998 to 1999, he was a Design Engineer with Ecostar Electric Drive Systems and Ford Research Laboratory, where he was a member of the Electric, Hybrid, and Fuel Cell Vehicle Development Programs. From 2001 to 2006, he was with the Department of Electrical Engineering, United Arab Emirates (UAE) University, Al Ain, UAE, as an Assistant Professor. In 2006, he joined the Department of Electrical Engineering, American University of Sharjah, where he is currently an Associate Professor. His primary research interests are in the areas of power electronics and their application to power systems, adjustable-speed drives, and alternative energy vehicles. He was a recipient of the Best Teacher Award from the College of Engineering, UAE University, for the academic year 2002 and 2003.